Challenges and Opportunities for Subsonic Transport X-Plane Acoustic Flight Research

Russell H. Thomas[1]
NASA Langley Research Center, Hampton, VA 23681 USA

Yueping Guo[2]
NEAT Consulting, Seal Beach, CA 90740 USA

Ian A. Clark[3] and Jason C. June[3]
NASA Langley Research Center, Hampton, VA 23681 USA

Aircraft system noise aspects of experimental aircraft acoustic flight research are analyzed. Experimental aircraft are seen as a key development step toward the introduction of a full scale low noise subsonic transport in the future, especially when considering an unconventional aircraft configuration integrating a range of advanced noise reduction technologies. Possible design scenarios for an experimental aircraft are considered where the scale of the experimental aircraft relative to the future, full scale aircraft is likely a major cost driver. Aircraft system noise predictions are presented for a NASA modeled Mid-Fuselage Nacelle subsonic transport concept. The predictions are made for the total airframe system noise at 100, 50, 25, and 12.5% scale of the full scale, future version of the concept, both without and then with a set of noise reduction technologies. The noise reduction technologies include the dual use fairing of the Krueger flap, the continuous mold line for the trailing edge high lift flap, and the pod gear concept for the main gear. The predictions are treated as simulations of flight test measurements of an experimental aircraft that are then processed to full scale as flight data would be. The analysis shows that the combined impact of frequency shift, atmospheric absorption, and background noise cutoff is to establish a realistic upper limit on useful frequency from the experimental aircraft noise. The implications for instrumentation requirements are also noted for high frequency, as well as for the challenge of identifying sources that are reduced significantly by the proposed noise reduction technologies. For the experimental acoustic flight research to be most useful for the objectives of improving the prediction of the future full scale aircraft, it is indicated that the scale should be above 75%. As the demonstrator scale approaches 50%, the limitations become more severe for direct impact to the prediction of the full scale future concept.

I.   Introduction

THE NASA Aeronautics Research Mission Directorate (ARMD) has set aggressive aircraft system level goals for fuel burn, emission, and noise reduction with the aim of developing the technology solutions that, if implemented, can reduce the negative impacts of aviation on communities and the environment. In addition, realizing these goals would be a key enabler to sustainable growth of the air transport system and, as a result, the economy. Aeronautics research focuses on innovating and developing technologies targeted for implementation across generations of aircraft from Near Term to Mid Term (2025-2035) and Far Term (beyond 2035). The concept of a notional vision vehicle is a model of the integration of a portfolio of technologies, engine, and airframe representative of the future vehicle at full scale. The performance of the vision vehicle can be predicted and measured relative to the aircraft system level goals and then updated as system level prediction methods are improved, integrated technology demonstrators produce new information, or as the modeling of the vehicle concept

---

[1] Senior Research Engineer, Aeroacoustics Branch, MS 461, AIAA Associate Fellow, Russell.H.Thomas@NASA.gov
[2] NEAT Consulting, 3830 Daisy Circle, Seal Beach, CA 90740, AIAA Associate Fellow
[3] Research Engineer, Aeroacoustics Branch, MS 461, AIAA Member

itself is improved. The prediction of the aircraft system level noise has been a particular challenge, and focused research has been going on at NASA for almost twenty years to improve the ability to predict future advanced technology aircraft concepts, especially with unconventional aircraft configurations that introduce advantageous propulsion airframe aeroacoustic (PAA) integration effects [1]. These favorable PAA effects together with the technologies that enhance the noise reduction from PAA effects have been shown to be critical to low noise advanced concepts [1, 2]. In fact, PAA effects are the single largest differentiator between vision vehicle concepts that are able to reach the upper end of the Mid Term noise reduction goal of 42 EPNL dB cumulative below the Stage 4 regulatory limit or the Far Term goal range from 42 to 52 EPNL dB cumulative [3]. As part of recent NASA projects, the prediction of the aircraft system level noise has been investigated for the portfolio of vision vehicle concepts of the Mid Term generation [3, 4], and initial technology roadmaps have been developed [5, 6] for the Far Term noise goal of 42-52 EPNL dB cumulative below the Stage 4 level.

Ultimately, it is industry's role to integrate these technologies on future aircraft products. However, the development by industry of an all new commercial transport is typically a multiyear venture that can require a multibillion dollar investment before the first aircraft flight. For this reason, a full scale prototype of an all new aircraft is unlikely, particularly one with both a range of new technologies and an unconventional configuration. Also unlikely is that the vision engine for a vision aircraft will be available in time for integration with the prototype aircraft. Therefore, an important step forward is the demonstration of key technologies and configurations, in flight, as part of the process of maturing technology, reducing uncertainty of performance, and developing manufacturing and implementation solutions. Toward this end, the ARMD has recently initiated research that may lead to demonstrator X-plane flight research [7]. Particularly for aircraft system noise, the configuration of the aircraft is itself a key technology because of the implications for the PAA effects, in addition to engine and airframe technologies that are also important contributors to total aircraft noise.

The most likely scenario is that an X-plane demonstrator must be a carefully designed vehicle using a commercial-off-the-shelf engine that is of a technology type representative of the vision engine. The demonstrator will be focused on demonstrating certain key technologies, including configuration, and on acquiring information, in a carefully designed flight research test, that is most valuable for understanding and validating performance of the selected key technologies as well as for improving the predictions (reducing uncertainties) of the performance of the vision vehicle.

Within this framework and focusing on the acoustics, this paper will discuss and analyze the key issues for the formulation of X-plane demonstrator aircraft research including vehicle scale, configuration PAA effects, noise reduction technologies, and the low speed flight testing of a demonstrator vehicle to support useful acoustic flight research.
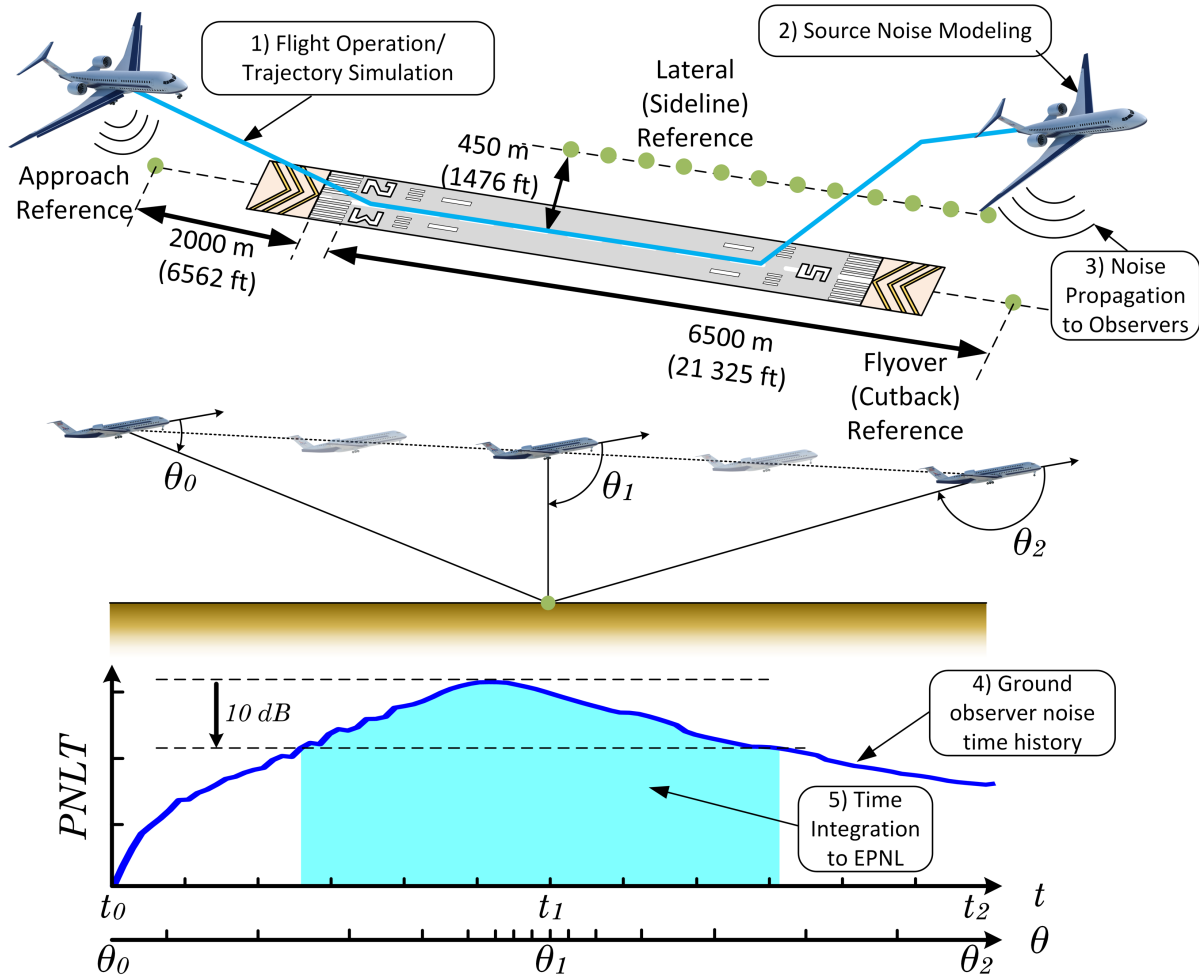
II.   X-plane Acoustic Flight Research Formulation

A. X-Plane Acoustic Flight Research Framework

As mentioned above, X-plane research is focused primarily on demonstrating the impact of key effects and technologies and on acquiring information from these key technologies that is used to improve the prediction of the full scale vision vehicle. For the acoustics of the vision vehicle, this initially involves the prediction of the conditions for noise certification. The conditions for certification are very useful because they encompass a wide range of low speed operations of the vehicle from approach to landing and takeoff and, therefore, represent those aircraft conditions that primarily impact community noise. It is important to note that the X-plane itself is not going to be noise certified nor is acoustic flight research expected to duplicate certification conditions exactly. However, the X-plane acoustic flights should be designed around those operations and conditions that will obtain the best, most relevant information in order to improve the prediction of the vision vehicle. For these reasons, the noise certification procedures are relevant and will be referred to throughout the paper.

An overview chart of the prediction process for noise certification is shown in Fig. 1. Specifically, the noise predictions for the vision vehicles follow the certification rules found in the Code of Federal Regulations (CFR) Title 14, Part 36 and illustrated in the figure. Part 36 defines specific operational parameters for each of the three certification points. For separate procedures at each of the three certification points, the Effective Perceived Noise Level (EPNL) dB is predicted for the aircraft. The cumulative noise is the addition of the EPNL of the three points. The cumulative noise is referenced relative to the certification level required by Part 36, currently Stage 5 as of January 1, 2018, and is a function of aircraft weight and the number of engines. The cumulative noise below the regulatory limit is typically the final noise metric reported.

Several observations relevant to an X-plane demonstrator of an advanced aircraft concept can be made in reference to the certification procedures. On a 3-degree glide slope to landing, the aircraft is at an altitude close to 400 ft. This is the closest distance to the microphones. For the flyover point, advanced aircraft with improved high lift can be as high as 2500 ft over the flyover point [3]. Also, the lateral point is measured at an off-center azimuthal angle relative to the aircraft (azimuthal angle is from wing tip to wing tip) in contrast to the other points that are directly underneath the aircraft. For all points, the EPNL metric is computed as a time integral of the tone corrected perceived noise level (PNLT) as the aircraft flies over and requires the noise to be measured over a wide range of polar angles (from nose to tail of the aircraft). Certification metrics require the one-third octave spectrum from 50 Hz to 10 kHz. Together, these requirements typically characterize the aircraft noise including human perception factors. At the same time, these parameters set up a number of challenges for an X-plane demonstrator, especially if scaled down from the vision vehicle.

Fig. 1 Noise certification flight paths and metric definitions used in the system noise assessment process. (Definitions guided by the Code of Federal Regulations (CFR) Title 14 Part 36.)

B. X-Plane Acoustic Flight Research Formulation Model

The introduction above has already mentioned several topics that are closely interrelated and form the elements that must be addressed in the formulation of the acoustic flight research of an X-plane. Fig. 2a provides a model to illustrate and discuss how these topics and others are part of this formulation process for the scenario where the acoustic technical objectives are a primary driver of the X-plane scale and technology selection.
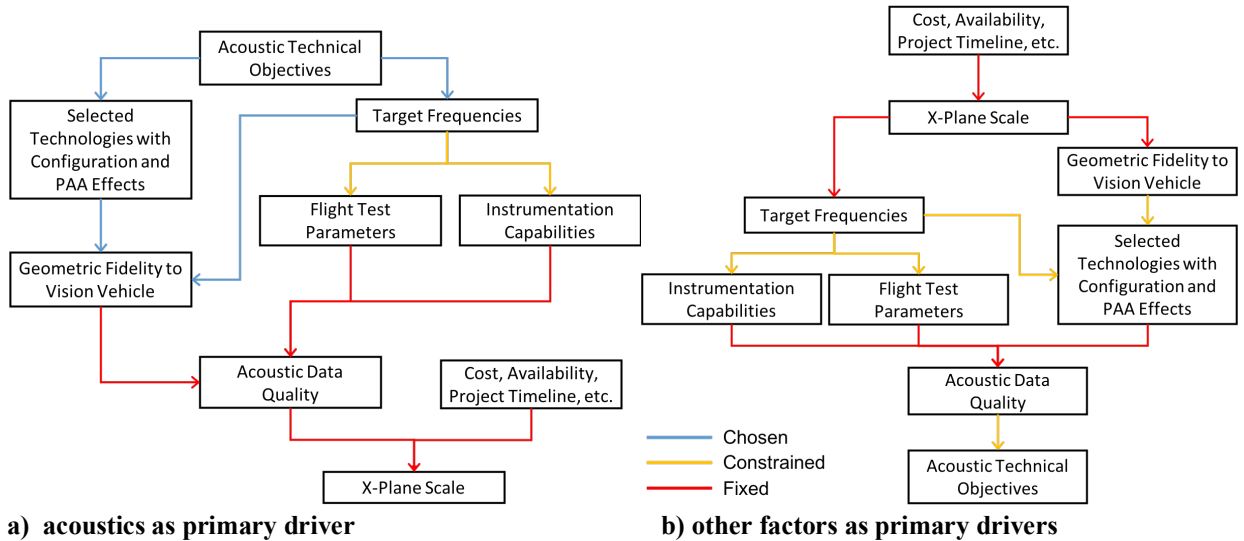
a) acoustics as primary driver   b) other factors as primary drivers

Fig. 2 Acoustic flight research formulation model for the scenario a), where acoustics requirements are a primary driver in the determination of the X-plane scale and design and b), when other factors have already determined the X-plane scale.

Figure 2b illustrates the formulation process for the scenario where other factors have already determined the X-plane scale factor. In this scenario, acoustics may still influence selection of some of the key technologies and the geometric fidelity. Given that the scale has already been imposed, the primary outcome of this scenario is to determine what acoustic objectives can still be accomplished and what capabilities (instrumentation and flight test matrix) are needed to do so. Another possible outcome is to develop alternatives for the acoustic technical objectives that might be achieved.

From an acoustics point of view, ideally, the process is used in a proactive way to determine the best scale factor for the configuration, PAA effects, and selected technologies. This approach would achieve the highest impact on the overall objective of predicted noise performance of the vision vehicle with greatest fidelity and minimized uncertainty. This proactive approach could also result in a direct demonstration of an X-plane that could meet the noise goal.

In either scenario, the scale of the X-plane is certainly one of the key results from the analysis in this formulation.

C. Acoustic Technical Objectives

Specific acoustic technical objectives must be related to one or both of the two overall objectives:

- Improve the prediction of the vision vehicle noise by improving and validating prediction methods for selected integrated technologies and PAA effects,
- Improve the prediction of the vision vehicle noise by directly scaling X-plane measurements for selected integrated technologies and PAA effects.

Improved prediction means the ability to predict integrated technologies or effects more directly and with higher fidelity (to physical mechanisms) than previously possible and, therefore, with reduced uncertainty to the prediction.

Starting with these two overriding objectives, specific objectives must be developed because of the significant impact that these may have in the design process. The development of these specific objectives is left to the implementation of the design process for a particular X-plane concept.

D. Aircraft Configuration and Selected Technologies

As discussed in the introduction, the PAA integration effects that result from aircraft configuration have been shown to be the single largest differentiator between vision vehicle concepts that are able to achieve the NASA Mid Term and Far Term noise goals and those that do not meet the goals. Therefore, acoustic flight research should include quantification of these effects, again in ways that can be applicable to the prediction of the vision engine on the vision vehicle. Some of these will be mentioned in Section V.A.

PAA effects introduce very strong directivity both in the polar angle, which is often measured in wind tunnel tests, and also in the azimuthal directivity angle, which was has been shown to be an important aspect of achieving

low noise aircraft goals [1, 2]. Azimuthal directivity of PAA effects is a critical measurement to include because it has a strong effect on the lateral certification point [1-3] and on the ground contours of noise that are a broader metric of noise impacting population in larger areas surrounding airports [8].

Many technologies have been studied for integration into NASA's advanced aircraft concepts. Some examples are included in the studies already referenced [1-6]. Each technology will have noise reduction with spectral and directivity characteristics when they are integrated into or added onto the X-plane. The measurement challenge is to identify the selected technology sufficiently enough to support the prediction or direct scaling to the vision vehicle where the measurement now includes flight effects and integration effects.

E. X-Plane Geometric Fidelity to the Vision Vehicle

Geometric fidelity to the vision vehicle is an issue that arises due to the demonstrator purpose of the X-plane. Even if the X-plane is a 100% scale of the vision vehicle, choices are likely to be made, due to cost or the use of off-the-shelf components, that reduce the geometric fidelity of the airframe components of the vehicle compared to those on the vision vehicle. These geometric fidelity issues are likely to have a significant impact on the acoustic levels and characteristics of the components that, in turn, can impact the accomplishment of the acoustic technical objectives.

For similar reasons, based on any overall dimension, the noise of a Boeing 737 is not scalable to match the noise of a Boeing 777. While the configuration is similar, the designs, detailed dimensions, complexity of certain components, and noise source ranking are different enough so as not to be scalable. The 737 could certainly be used to demonstrate the effectiveness of a noise reduction technology but the resulting noise impact would not be simply scalable up to a 777.

F. Target Frequencies

FAA certification requires aircraft noise to be measured in one-third octave bands from 50 Hz to 10 kHz. Frequencies from 2 kHz to 4 kHz have a higher weighting due to human perception factors and, therefore, more impact on the EPNL metric. The acoustic frequencies of the noise of a scale model are inversely proportional to the scale factor. Therefore, in general, a small X-plane will generate lower noise levels due to smaller dimensions, lower lift, lower weight, and lower thrust. The X-plane noise must be measured to higher frequencies if the X-plane noise is to be scaled up to predict the noise of the vision vehicle. This fundamental relationship has many implications, one of which is how the atmosphere dissipates noise as a function of frequency and distance as the noise propagates to the measurement location.

G. Acoustic Flight Test Conditions and Variables

There are many possibilities for operation of the X-plane in an acoustic flight research campaign. For example, higher noise levels can be measured if the vehicle is flown closer to the microphones. However, flying too close to the microphones can have several counterproductive impacts on data quality including a slew rate (how fast the aircraft passes the microphones) that is too high or a measurement that is no longer in the far field of the aircraft. Also, there are many constraints to ensure safety. The X-plane may not be able to fly safely on approach to landing at a desired altitude, control surface allocation, or velocity.

Background noise is another consideration, especially when considering the range of frequencies, angles, and propagation distances required. Certification calls for a signal 20 dB above the background, a value that may be difficult for many test points. Background noise can vary with test site, time of day and weather conditions, of course. Transients due to nearby extraneous noise sources must also be minimized or preferably eliminated.

This is by no means an exhaustive list of important considerations; it is meant only to be indicative.

H. Acoustic Instrumentation Capabilities

Aircraft installed acoustic instrumentation can include unsteady pressure sensors and microphone phased arrays. Ground based acoustic instrumentation should include arrays of single microphones (such as certification type microphones) and microphone phased arrays. Each type of system has critical signal-to-noise criteria. The number, frequency range, array design, placement, installation details, calibration procedure and microphone type for all of these systems have implications for achieving the objectives. It is likely that the challenges discussed in following sections will result in increased requirements, particularly on the phased array system. With this brief mention, more discussion of instrumentation issues will be made in Section VI.C. after the aircraft noise predictions have been made to provide more context for instrumentation requirements.

I. Acoustic Data Quality

This is a filter to determine if the design decisions and available capabilities combine to result in the ability to identify the intended noise source with sufficient signal-to-noise ratio, frequency range, and azimuthal and polar angular range in order to accomplish the intended purpose(s) of the data, e.g., determining the impact of a technology, comparison with predicted results, or scaling an absolute noise result or a noise difference up to the full scale vision vehicle.

For the purposes of the acoustic flight research, the measured data are processed following the procedure in Fig. 3. This procedure is used for full scale testing or scaled demonstrator testing, differing only by the scaling on size.
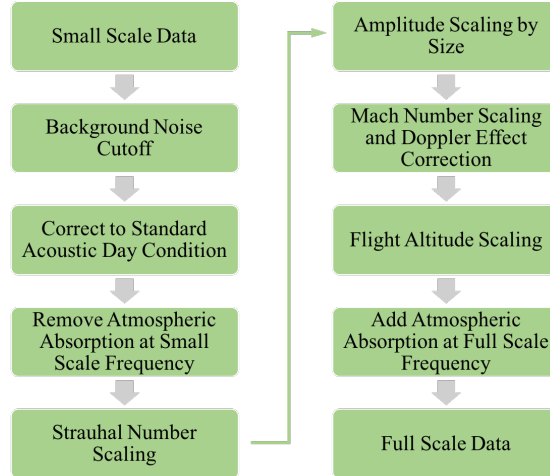
Fig. 3 Noise data processing to correct to equivalent conditions and also to scale to full scale data.

In the example case studies used in following sections, many of the issues mentioned above in Sections II D. to I. will be quantified as the process is demonstrated, and more aspects will be identified. However, these topics are not addressed fully in this paper and are left to future work.

III.   Mid-Fuselage Nacelle (MFN) Concept Aircraft

For the purposes of illustrating the impact of the topics related to the decision process for an X-plane, the following sections will use, unless otherwise stated, the example of the MFN aircraft from the NASA portfolio of future concept aircraft. This section will show a brief description of the MFN as a reference to the calculations that follow. In effect, the MFN is used as a representative example of a vision vehicle. The MFN is a configuration change from the traditional engine-under-wing, has a very low noise level for the Mid Term and Far Term technology levels, and as a vision vehicle can include a broad range of advanced technologies that are likely to be applicable to other vision vehicle concepts.

The NASA MFN concept was originally included in the Boeing work on the Advanced Vehicle Concept contract in 2011 [9] with Boeing identifying this as the -0027A concept. Boeing's concept was a double deck aircraft for 228 passengers and a design mission of 8000 nautical miles. The engines were mounted from the fuselage (pylon structure attaching through the floor of the top deck) and with the inlet of the engine over the trailing edge of the main wing. The system noise predicted by Boeing was 28.0 EPNL dB cumulative below Stage 4, showing the significant advantage from the PAA effects of the over-the-wing engine mounting.

To NASA systems analysts this concept represented a revolutionary design, yet still of a tube-and-wing architecture, that incorporated favorable PAA effects without a transformational change to an HWB configuration. Again, favorable PAA effects are essential to an aircraft with advanced engine and airframe technology to achieve the NASA Mid and Far Term noise goals.

In 2014, NASA and Boeing collaborated on a system noise prediction of the -0027A concept adding potential noise reduction technologies and redesignated the concept as the B27. The result was a cumulative noise level of 35.9 EPNL dB below Stage 4 [10]. Figure 4 shows a rendering of the B27 concept as described in [10].

As part of the final assessment of the Mid Term aircraft concepts, the NASA MFN for the 301 passenger class was modeled by NASA as part of a thirteen vehicle portfolio, all with consistent technology assumptions for the Mid Term timeframe. The modeling of the aircraft and the fuel burn and emissions reduction assessments were reported

by Nickol and Haller in 2016 [11]. Updated modeling results of the MFN are shown in Table 1 with an artist rendering in Fig. 4 [6]. The designation MFN301-GTF-B was used in Ref. 6 to indicate it was a 301 passenger class vehicle with a NASA-modeled, geared ultra high bypass ratio engine, and it was the baseline for the study reported in Ref. 6. For system noise, the MFN assessed at 33.9 EPNL dB cumulative below Stage 4 [3].

Table 1 Modeling results for the NASA MFN concept for the Mid Term technology generation (from Ref. 6).

	Units	MFN301-GTF-B
		FLOPS
TOGW	lb	544,747
OEW	lb	262,988
Payload	lb	118,100
Passenger Number		301
Range	nm	7500
Total Fuel	lb	163,659
Block Fuel	lb	147,366 (- 46.8% relative to 777-200LR-like)
Wing Area	ft^2	4,891
Wing Span	ft	208.6
Aspect Ratio		11.0
Wing Loading	lb/ft^2	111.4
Cruise Mach		0.84
Start of Cruise Lift/Drag		23.8
Landing Field Length	ft	5,598
Thrust per Engine	lb	65,500
Fan Diameter	in	149.2

Fig. 4 Artist rendering of the double deck NASA MFN vision vehicle.

## IV.   Some Fundamental Issues for Acoustic Flight Testing

A. Differences Between Acoustic Wind Tunnel and Flight Testing

The scale of the demonstrator X-plane relative to the vision vehicle is an overriding factor in both the cost of the demonstrator as well as the implications for the acoustics. Scale of a wind tunnel model is also a critical factor in the design of an aeroacoustic wind tunnel test. However, the range of model scale is completely different between a wind tunnel model and an X-plane. It is common to test models in aeroacoustic wind tunnels at scales of 3 to 10%, for example. However, wind tunnels also allow microphones to be placed relatively close to the model, within 25 feet for example, and wind tunnels have controlled environments with stable velocities and a fixed position for the model.

Flight testing has a very different paradigm and sets up an interrelated set of challenges that are a strong function of scale. Scale factor changes both amplitude and frequency so that a scaled down vehicle has a lower noise amplitude with a higher frequency range compared to the noise of the full scale vision vehicle. The distance between the microphones and aircraft that are typical for commercial transport noise certification conditions can vary from a minimum of about 400 ft at approach and between 1800 to 2500 ft for lateral and flyover points, respectively, for the NASA-modeled Mid Term generation.

The noise generated by each of the aircraft noise sources spreads spherically from the source to the geometric far field, and from this spherical spreading, the noise amplitude decreases with distance. The atmosphere also dissipates or attenuates noise as a function of frequency as the signal propagates with distance. This is called atmospheric absorption. Higher frequencies absorb much more rapidly with distance as compared to lower frequencies. For the vision vehicle at 100% scale, the signal that is emitted from the vehicle will be reduced from spherical spreading and, in addition, will be attenuated by the frequency-dependent atmospheric absorption with propagation to the microphone. As vehicle scale goes down, frequencies go up and the atmospheric absorption becomes an even greater challenge.

Quantification of these effects is shown in Fig. 5. The effect of spherical spreading is shown with the curve marked "No Absorption," and amplitudes at all frequencies are reduced equally by spherical spreading. What is seen is a 6 dB decrease with each doubling of distance. In contrast, atmospheric absorption is a strong function of frequency, and Fig. 5 shows how dramatically the amplitude is reduced by absorption as frequency increases. For a 50% scale vehicle, if the objective is to measure 100 Hz to 20 kHz in order to be able to scale to the noise of the 100% vision vehicle (50 Hz to 10 kHz), Fig. 5 shows that the magnitude of the corrections for absorption become as large as 35 dB beyond 10 kHz. This is for the minimum propagation distance of 400 ft.
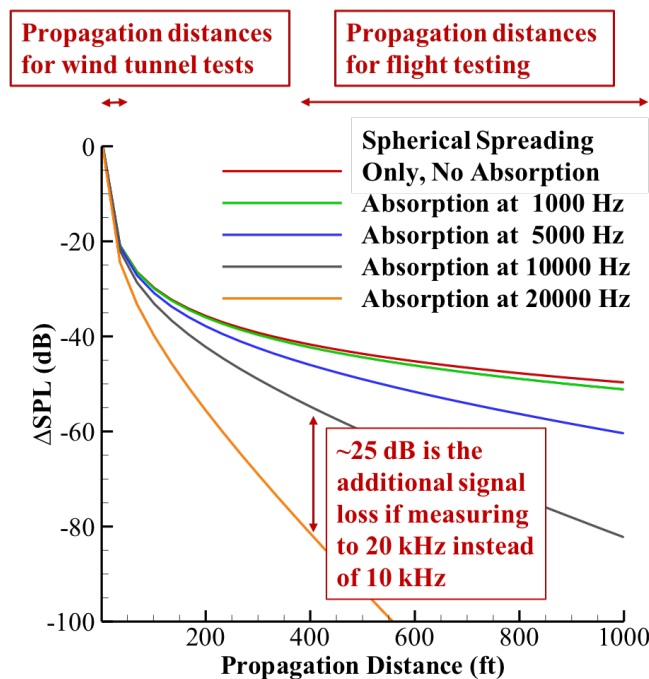
Fig. 5 The dependence of noise amplitude on distance and atmospheric absorption.

In addition, absorption is a function of ambient temperature, relative humidity, and pressure to a lesser extent. Fig. 6 shows the effect on absorption of an 18 deg F change in ambient temperature. Even for a full scale vehicle, correction of the measurements to a standard day temperature (multiple measurements taken at different temperatures and then corrected to the same temperature) require significant change in values, up to 10 dB/1000 ft, over frequencies of 6 to 10 kHz.

To show the impact of absorption at the aircraft level, the total airframe noise of the MFN (Krueger flap, trailing edge flap, nose and main gear) is predicted using the methods for airframe noise that are currently in the research level version of the Aircraft Noise Prediction Program (ANOPP); GuoLG-v2 [12], GuoLE-v2 [13], and GuoFlap-v1. The conditions for the predictions are approach for noise certification with a minimum distance from aircraft to microphone of 396 ft corresponding to the aircraft directly overhead of the microphone, at a polar angle of $\theta = 90°$.

The results are shown in Fig. 7 for the 100% vision vehicle and for three scaled demonstrators, with and without absorption.
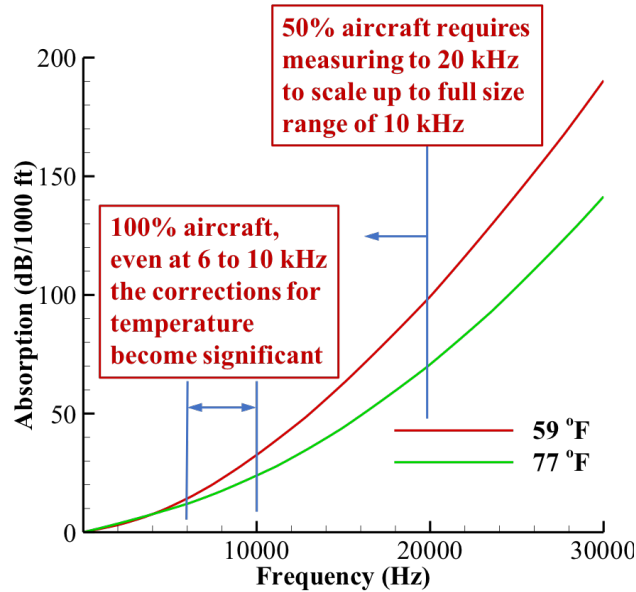

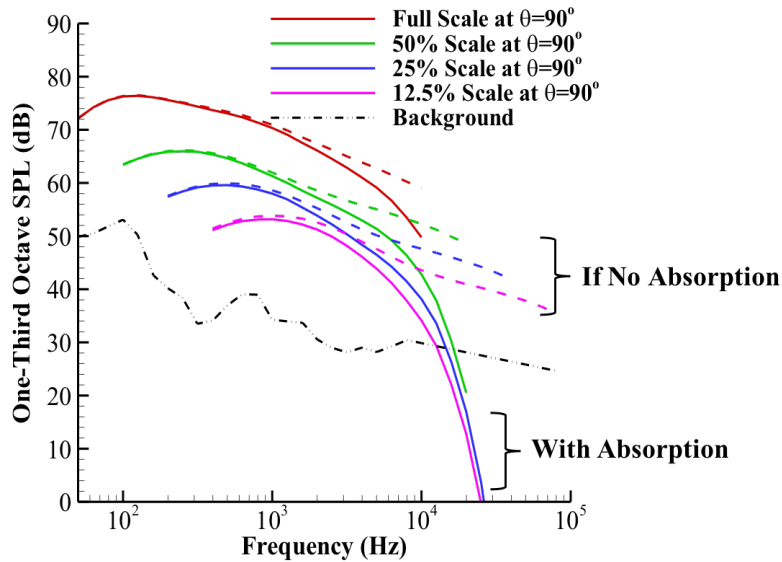**Fig. 6 The effect of temperature on atmospheric absorption.**

Fig. 7 The effect of absorption for total airframe noise of a 100% vision vehicle and three scaled X-Planes, propagation length of 396 ft.

B. Background Noise

Background noise levels are an issue for both wind tunnel and flight acoustic testing. For acoustic flight testing, background noise represents a floor below which the test acoustic signal is lost or cutoff. This cutoff is therefore a part of the data process of Fig. 3. Due to the propagation distances and the atmospheric absorption, the background noise level is likely to be a critical level. Figure 7 shows a representative level of background noise that was obtained from a set of available measurements provided from recent NASA acoustic flight tests conducted at the Armstrong Flight Research Center (on the adjoining Edwards Air Force Base) and at the Wallops Flight Facility. Figure 8 shows the three sets of data, a single microphone at Wallops and three microphones at Armstrong for two different test days. Note that the Wallops data were limited to 5 kHz and the Armstrong data were limited to 10 kHz. A reasonable extrapolation is made above 10 kHz; however, this is precisely the range of great importance for scaled vehicle testing. The wind screen is used to attenuate the impact of wind on low frequencies; however, the wind

screen has been shown to also attenuate the high frequencies. Clearly, some dedicated measurements should be made for background noise including consideration of the wind screen attenuation and weather condition variability.
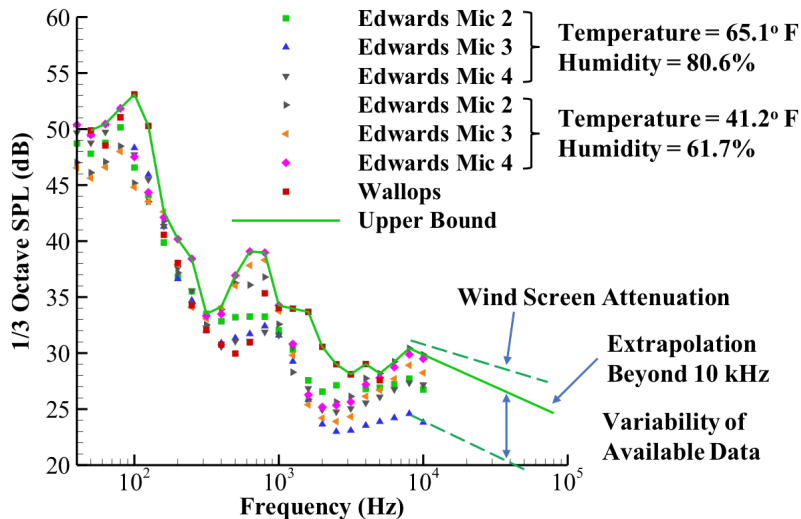

Fig. 8 Available background noise from two NASA acoustic flight tests.

## C. Atmospheric Absorption Prediction Uncertainty

It has already been shown that for scale vehicles, the effects of atmospheric absorption greatly impact the spectral levels. Even for a full scale vehicle, the measurement and processing of data above 6 kHz requires the need for increasingly large corrections to the measured data in order to correct data from multiple tests to equivalent atmospheric conditions. This correction requires knowledge of the atmospheric pressure, temperature, and humidity along the path from the source to the observer, as well as the path length. A model is then applied to estimate the atmospheric absorption effect in the data using these atmospheric properties. The modeled absorption is removed from the spectral levels at the observer, yielding an estimate of the lossless spectrum at the observer. This can either be propagated back to the source by taking into account spherical spreading, which then allows for development of source models, or it can be compared to other test flights by adding absorption back into the spectrum based on the standard atmospheric conditions chosen for comparison. By removing the atmospheric absorption, there is some uncertainty introduced from imperfect knowledge of the test atmospheric conditions and path length, as well as differences in the atmospheric absorption model and the true physics of the problem.

For a scaled X-plane, uncertainty in spectral levels from removal of atmospheric absorption is typically larger than for a full scale aircraft. This is due to the fact that calculation of the atmospheric attenuation generally becomes more sensitive to uncertainties in the atmospheric properties as well as path length with increasing frequency. A further complication arises if it is desired to extrapolate the measured X-plane data (or predictions from the X-plane data) to the full scale vision vehicle, for instance, through the process outlined in Fig. 3. This has to do with magnification of the uncertainty in the scaled X-plane spectral levels as that uncertainty is propagated through the process for scaling to the vision vehicle.

It is then of interest to identify ways that the uncertainty in the atmospheric absorption can be minimized when comparing two tests taken at different atmospheric conditions. With respect to the inputs of the models, improvements can be made when higher quality transducers are used to determine the atmospheric properties, and when the spatial resolution of these properties as a function of altitude is improved. The uncertainty related to the atmospheric absorption model can be reduced by choosing the model with rigorous theoretical development and widest experimental validation.

Over the past half century, many models have been proposed for estimating atmospheric absorption, a detailed history of which can be found in Bass et al. [14]. While the theory for absorption from classical thermoviscous effects had been well defined by the beginning of this period, there was significant maturation of the understanding of the role of molecular relaxation on absorption. Consequently, the differences between the models have generally centered on the molecular relaxation process. One of the earlier models that has seen considerable use is the Society of Automotive Engineers (SAE) ARP866A standard [15], which is the method specified by FAR Part 36 governing corrections of certification flight tests to the regulated atmospheric conditions. This method is used here for consistency with certification procedures, as well as the ease of application of the method to one-third octave band

spectral levels. However, this model only incorporated relaxation losses from O_2. It did not consider the additional effect of atmospheric pressure on absorption. Later experimental research showed that the relaxation process for N_2 in the atmosphere also produced a sizeable contribution at certain atmospheric conditions. The incorporation of this fuller theoretical backing, and a rich validation of the theory has culminated in the ANSI S1.26-2014 standard [16]. A comparison of these two standards can be seen in Fig. 9, showing the difference in the atmospheric absorption predicted by the two methods, over the range of atmospheric conditions allowed by certification at 4 kHz, over a path length of 1000 ft. This provides an illustration of the errors that can be incurred by using a model that neglects some of the physics of the problem.
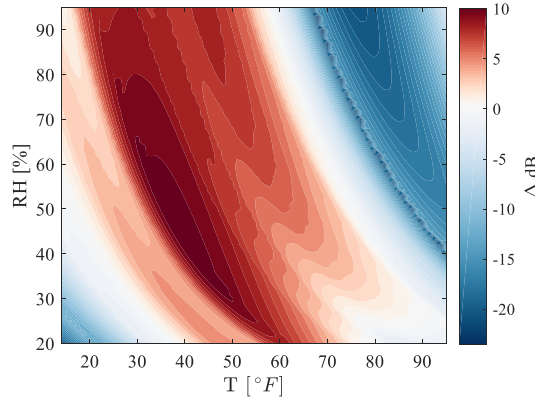
Fig. 9 Plot showing the difference in atmospheric attenuation between the ANSI 2014 standard and the ARP 866A standard at 4 kHz and a path length of 1000 ft for a range of temperature (T) and relative humidity (RH) at standard pressure.

An additional source of uncertainty is application of attenuation coefficients to a frequency band. As the frequency increases, the variation of atmospheric attenuation coefficients for each of the frequencies contained in a standard fractional octave band increases. The SAE standard attempted to take this into account by using the fractional octave center frequency at and below 4 kHz, while using the lower edge band frequency for bands otherwise. This attempts to account for the high frequency roll off of the spectral levels, which implies that most of the energy in the band is biased toward the lower edge of the band. More sophisticated approaches have been suggested, such as breaking the fractional octave band into even smaller subbands and determining attenuations for each subband [17]. However, these methods make assumptions about the distribution of the energy within the subbands. For flight tests, this problem can be avoided entirely through storage of narrowband spectra, which is the natural extension of the subbanding technique. Data should only be converted to wideband as a final step.

With respect to the best available atmospheric absorption model, the ANSI standard, the accuracy of the standard is quoted in percent of the attenuation per unit distance. For the range of atmospheric parameters and frequencies that are typically seen in flight testing this is stated as ±10%. As it is specified as a percentage, the uncertainty will be minimized at the atmospheric conditions which produce the minimum attenuation. However, this region changes with frequency, so the desired atmospheric conditions are likely to be a function of the X-plane scale. The dependence of the absorption coefficient on atmospheric conditions is shown for 6 kHz and 24 kHz in Fig. 10.
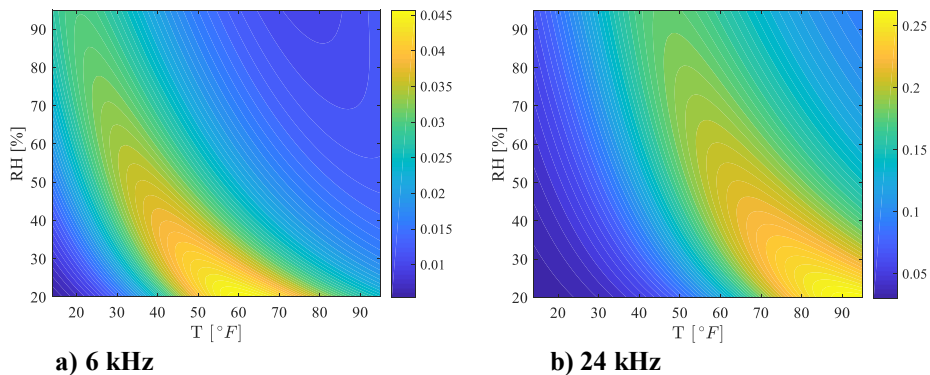
	a) 6 kHz	b) 24 kHz

Fig. 10 Comparison between the predicted atmospheric absorption coefficient [dB/ft] at a) 6 kHz and b) 24 kHz using the ANSI 2014 Standard.

For a full scale feature at 6 kHz, it appears that higher temperatures and relative humidity are desired to measure the component. However, this is not the case for the same feature at 25% scale. For this reason, it is difficult to identify general atmospheric conditions that are suitable for minimizing atmospheric absorption uncertainty. However, once the vehicle scale and frequency range of the components are set, it is straightforward to identify atmospheric conditions to minimize uncertainty.

When considering how to minimize the uncertainty of scaling the X-plane data to a full scale vision vehicle prediction, there is minimal additional guidance apart from the strategies outlined above. The magnification of the uncertainty through the scaling process can be minimized by increasing the scale factor of the X-plane closer to the true size of the vision vehicle. Additionally, for small scale X-planes, the uncertainty can be limited by only extrapolating low frequency sources and effects for use in the prediction of the full scale vision vehicle.

V.   X-Plane Acoustic Flight Research Case Studies

A. Perfectly Scaled X-Plane Airframe

For the MFN as the example vision vehicle, consider the scenario where the vehicle is perfectly scaled down from 100% to 50%, 25% and finally to a 12.5% X-plane demonstrator vehicle. Perfect scaling of the vehicle means that the geometric details are maintained in perfect fidelity to those of the vision vehicle even as dimensions reduce with scale. This is practically an unlikely scenario, although it is useful as one limit of the design range. As a side note, geometric fidelity is also a very relevant issue for wind tunnel models where sufficient geometric fidelity (to the full scale) is often impossible to obtain on the smallest models and, at least, difficult and costly to obtain even on larger wind tunnel models (e.g., 10% or larger).

The results in Fig. 11 are predicted to be the "as-measured" noise at approach conditions for noise certification. Clearly the progressively decreasing noise amplitudes are seen as the model scale decreases. Fig. 11 also shows the progressively increasing frequency range, which results from the Strouhal number scaling in order to collect data in the correct range for extrapolating the small scale model test data to full scale. The noise levels drop to very low levels at high frequencies due to heavy atmospheric absorption. The amplitudes approach and then drop below the background noise. In Fig. 11, a typical ambient background noise taken at Wallops Flight Facility is used as an example. Day to day variability and even run-to-run variation in the background noise will be a reality, and this may further limit the upper useable frequency range. Yet another challenge is accurately measuring the background noise at the higher frequencies.
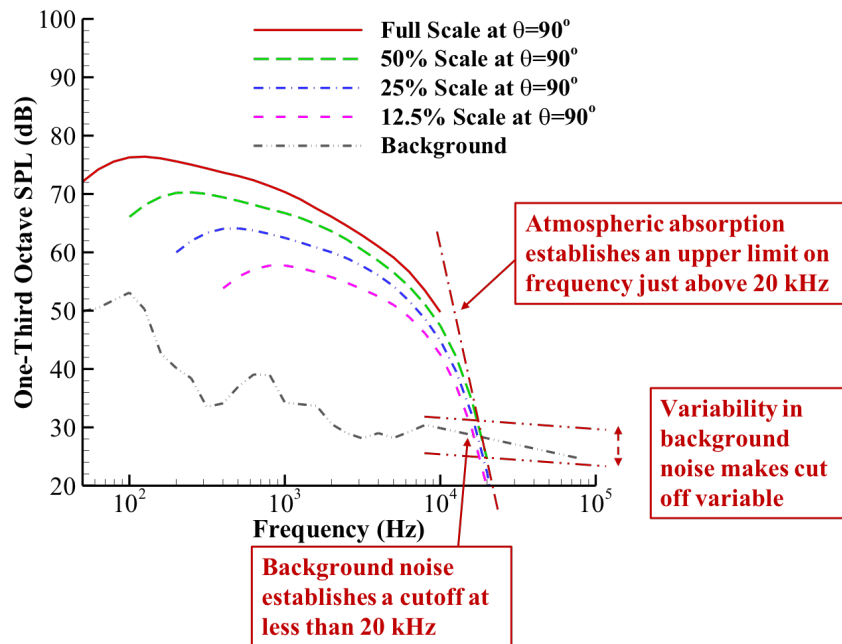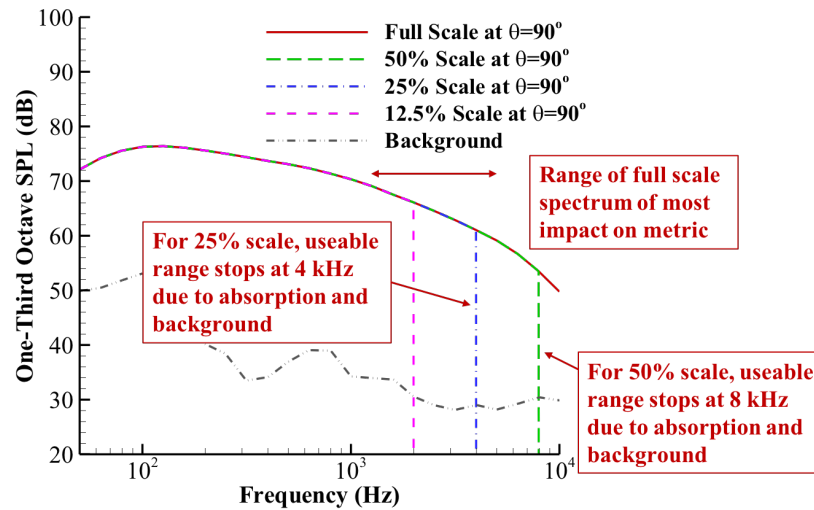

Fig. 11 Total airframe noise "as-measured" for the vision vehicle at 100% and three perfectly scaled X-planes, 90 degrees polar angle or 396 ft from the observer.

12

Extrapolating to the full scale vision vehicle requires processing the results from Fig. 11 by the method of Fig. 3. The results of this process are shown in Fig. 12.


Fig. 12 Full scale processed results for the perfectly scalable X-Plane case study results of Fig. 11.

The Effective Perceived Noise Level (EPNL) metric includes human perception factors that make the 2-4 kHz range the part of the full scale metric of most importance. Even widening out that range to just 1-5 kHz, the results of Figure 12 show that both of the smallest scaled X-planes would be missing parts of this most important range of the full scale spectrum, due to background noise cut off. For these reasons, and before considering other issues, the useable frequencies can be very limited for scaled demonstrator tests.

It is also noted that the results shown in Figs. 11 and 12 are for the polar angle of 90 degrees so that the propagation distance from the aircraft to the microphone is close to the minimum of 396 ft. At other emission angles, as the aircraft flies toward and then recedes from the microphone, the loss of signal from atmospheric absorption is even more severe because of the distance. An EPNL metric calculation requires a wide range of polar angles as the aircraft flies overhead in order to determine the 10 dB down points. At polar angles above and below the overhead of 90 degrees, propagation over longer distances will only diminish the useable frequency range from scaled demonstrators.

One example is shown in Fig. 13 for a polar angle of 122 degrees, as the aircraft recedes past the observer microphone. The propagation length is now 445 ft, and the effect of more atmospheric absorption is seen in Fig. 13 with lower levels. In addition, the background noise cut off is close to 15 kHz and in reality, to ensure good signal-to-background noise ratio, the frequency limit would be more stringent, perhaps 10-12 kHz would be the maximum allowable frequency at this angle.
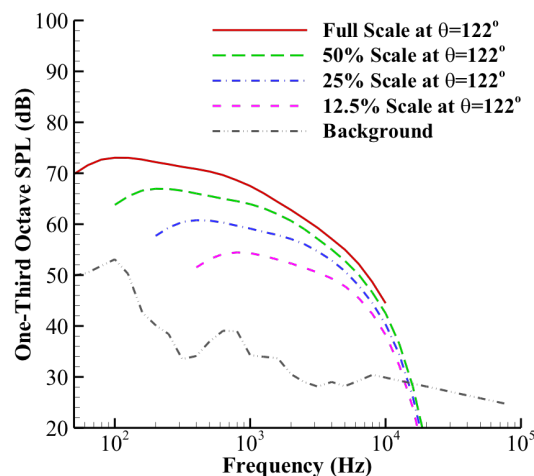
Fig. 13 Total airframe noise "as-measured" for the vision vehicle at 100% and three perfectly scaled X-planes, polar angle of 122 degrees or 445 ft from the observer.

B. Realistically Scaled X-Plane Airframe

The issues of geometric fidelity to the full scale vision vehicle are a practical and a cost constraint. In reality, a scaled demonstrator will likely have many fidelity compromises that can have significant impacts on noise. An easy example is that of the landing gear. The MFN vision has a six-wheel main gear. Even at a 50% demonstrator scale, it is likely to be prohibitive to fabricate a one-of-a-kind 50% six-wheel main gear with geometric fidelity perfectly scaled, as in the previous example. It is much more likely that cost and availability will drive the use of an off-the-shelf gear to match the weight of the demonstrator, a two-wheel main gear. This type of decision has implications for system noise as well as the demonstration of noise reduction technologies, in this case for the main gear, on the X-plane.

Consider the next case study of a realistically scaled X-plane where a two-wheel main gear replaces the six-wheel of the vision aircraft. In addition, due to smaller scaled dimensions the leading edge device and the trailing edge flap are also at reduced geometric fidelity, less complexity, as compared to the vision aircraft's airframe components. The Guo airframe models enable the prediction of the airframe's components at a complexity comparable to the scale factor. In this way, the airframe noise of scaled MFN demonstrators can be compared, first, at the minimum propagation distance of 396 ft, Fig. 14, as measured and then extrapolated to full scale, Fig. 15. As expected, at a longer propagation length, 445 ft corresponding to a polar angle of 122 degrees, the differences at full scale accentuate as shown in Figs. 16 and 17. For these realistically scaled X-planes, the reduced complexity results in lower noise levels that only further constrain the full scale extrapolation having already considered atmospheric absorption and background noise. At the 122 degree polar angle, even the 50% scale vehicle is beginning to be frequency constrained.
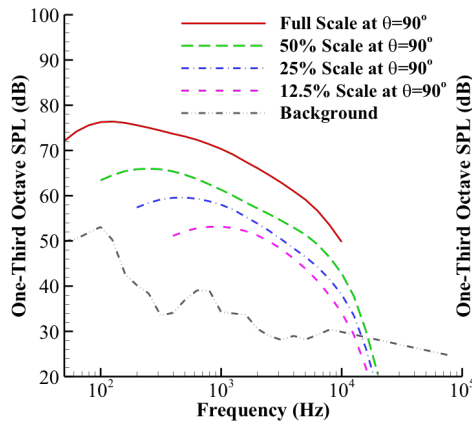
Fig. 14 Realistically scaled (reduced geometric fidelity) X-plane noise as measured, propagation length of 396 ft.
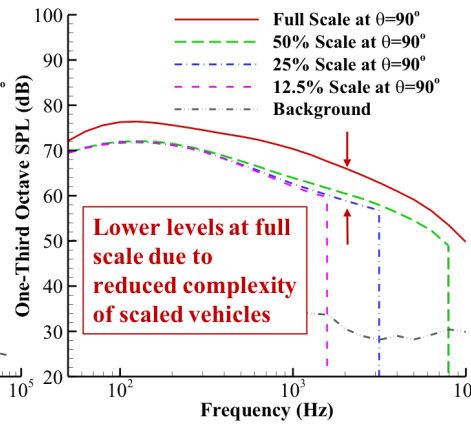
Fig. 15 Realistically scaled (reduced geometric fidelity) X-plane noise extrapolated to full scale. Vertical dash lines indicate the frequency cutoff.
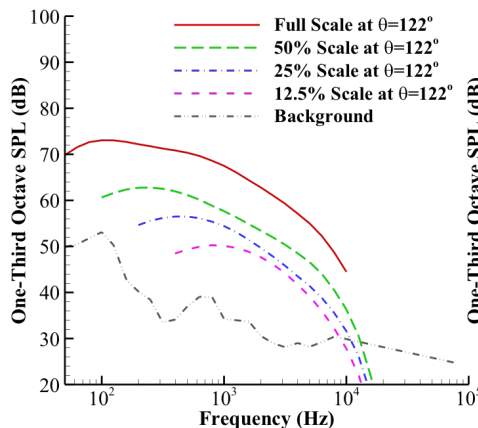
Fig. 16 Realistically scaled (reduced geometric fidelity) X-plane noise, as measured, propagation length of 445 ft.
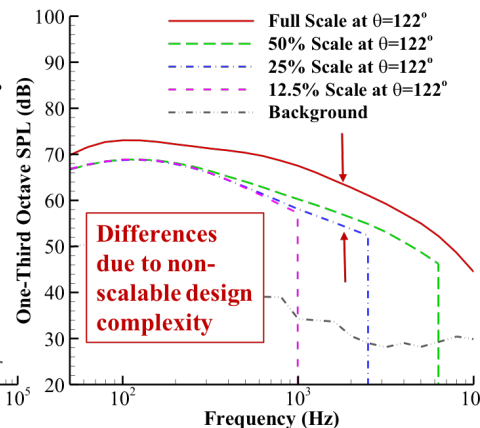
Fig. 17 Realistically scaled (reduced geometric fidelity) X-plane noise extrapolated to full scale, 445 ft. Vertical dash lines indicate the frequency cutoff.

14

VI. Opportunities for X-Plane Acoustic Flight Research

A. Propulsion Airframe Aeroacoustic Noise Reduction

It is known that engine noise has multiple sources, including the jet, fan, combustor, and turbine noise components. For the same engine-airframe configuration, these sources can have different shielding efficiencies, because of the differences in their respective source locations, directivities and coherences. Thus, the X-plane engines need to have not only all the major noise source components, but also the correct ranking order of the source amplitudes and the correct characteristics of the component noise such as the component directivity. If this is not the case, then the demonstration of engine and PAA related acoustics must be carefully planned to achieve an effective result for the vision vehicle.

The relative amplitudes between the jet noise and the aft fan noise serve as a good example to bring out the effects of source ranking order on the far field noise shielding. For this purpose, aircraft engines can be grouped into three types; first, the legacy engines with modest bypass ratio of nine or less that are on many aircraft currently in service; second, the next generation of engines that have recently been in production or are close to completion in design with high bypass (HBP) ratio between about 9 and 12; and, third, the ultra-high bypass (UHBP) ratio engines envisioned for the future with bypass ratios above about 12. This progression of engine architecture has profound impact on engine noise, as well as propulsion efficiency. In addition to the changes in the total engine noise levels, there is a significant change in the ranking order of importance between the major sources. In terms of the jet and the aft fan noise components, the increases in the engine bypass ratio progressively reduce the jet noise, by lowering the mixed velocity at the jet exit. This correspondingly increases the importance of the aft fan noise, both because of the relative amplitudes between the jet and the fan noise components, and because of the larger diameter and shorter length for larger bypass ratio engines, leading to higher fan noise source strength and less liner treatment.

To illustrate the effects of source ranking order between the jet and the aft fan noise components on the efficiency of engine noise shielding by the airframe, the three groups of engines are defined as jet-dominated for the legacy engines, equally important between fan and jet for the next generation of HBP ratio engines, and fan-dominated for the UHBP ratio engines. These are summarized in Table 2. To quantitatively describe the three types of engines, the definition of a dominant component means that its source amplitude is 4.8 dB higher than the other component, corresponding to an energy ratio of 3. Needless to say, the grouping of the engines by their respective bypass ratios and the number of 4.8 dB for the definition of the dominant component are both only for the convenience of the discussions here, meant only to illustrate conceptually the effects of noise shielding, and by no means intended as a formal classification of the engines and their noise components.

Table 2 Definitions and characteristics of engines.

Engine	Legacy	HBP	UHBP
Engine Definition	Currently in Service	Next Generation	Future Generation
Example	GE90	Trent 1000	Future GTF, ATF
Bypass Ratio	Below 9	9 ~ 12	Above 12
Noise Ranking Order	Jet Dominant	Jet-Fan Equal Importance	Fan Dominant

The noise reduction from the shielding effects for the three types of engines is illustrated in Figure 18 where the jet and the aft fan noise sources are modeled as two incoherent sources, with the aft fan noise source located at the engine exit and the jet noise source at 5 diameters downstream of the engine exit. In this hypothetical case, the engine exhaust is assumed to be mounted 0.8 diameters above the upper surface of the airframe and 1.0 diameters upstream of the aircraft trailing edge. To be clear, this hypothetical case is not relevant to the MFN but could be representative of other configurations. The figure plots the tone-corrected Perceived Noise Level (PNLT) as a function of receiving time for a typical flight path. The absolute levels are normalized to facilitate comparisons so

that the actual flight conditions are not relevant here, and the conclusions apply for all three certification conditions, namely, at approach, flyover and lateral operations. Four cases are shown in the figure; the solid red curve is for the isolated case, with no shielding, while the other three cases are with shielding, respectively, for the three types of engines, as indicated by the legend. The source levels for all four cases are normalized to be the same so that the differences in the plotted PNLT and the values of the EPNL, also given in the legend, are entirely due to the effects of the source ranking order and shielding effectiveness.

Clearly, because of the respective source locations in relation to the airframe, the aft fan noise is shielded more than the jet noise. This is demonstrated in Fig. 18 where the total noise reduction increases as the relative importance of the aft fan noise increases, from the jet-dominant legacy engine to the HBP ratio engines with equal importance between jet and fan noise sources, and then to the UHBP ratio engines with the fan noise dominant.
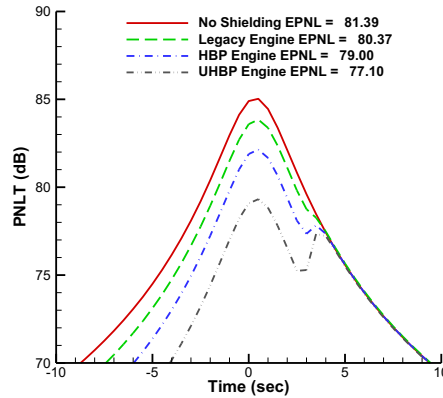
Fig. 18 Shielding effects for various engine types.

In addition to the source ranking order, many other factors can impact the noise reduction from shielding of engine noise, the component source directivity being one of them. This effect is illustrated in Fig. 19, which plots the PNLT and the corresponding values of EPNL for directional sources located at the engine exit to simulate aft fan noise. Four cases are plotted in the figure, all having the same source strength but with different directivities. Their respective peak radiation angles are given in the legend; the angle being measured is the conventional polar angle with zero being the upstream direction and 180 degrees being the downstream direction. As can be expected, the case of the most significant shielding is when the peak radiation is at 90 degrees, normal to the shielding surface, given by the red solid curve in the figure. The shielding benefit decreases as the peak radiation moves towards the aft quadrant with more radiation into the unshielded or direct radiation domain. The results in the figure clearly show the importance of the directivities; a variation of about 10 degrees can lead to a difference in EPNL between one and two decibels.
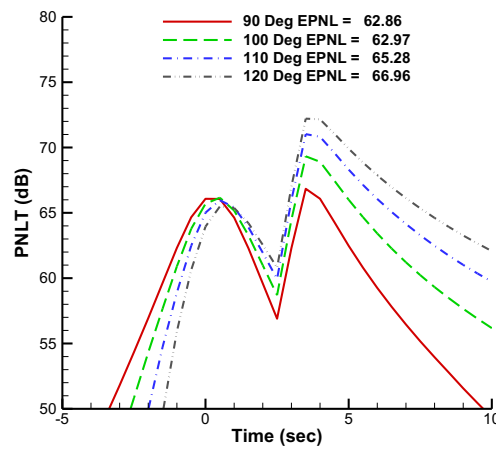
Fig. 19 Effects of source directivity on noise shielding.

The above two examples, respectively given in Figs. 18 and 19, clearly show the importance of engine source similarity in planning scaled demonstrator flight testing. In anticipating the use of UHBP ratio engines for future aircraft, the choice for the X-plane engines needs to have a sufficiently large bypass ratio so that aft fan noise is a major engine noise component, preferably the dominant component. It is recognized that currently available engines are not likely to exactly match the source ranking order and component directivity of future UHBP ratio engines, but the minimum requirement for the engine choice is the feasibility of component noise decomposition, either experimentally or theoretically or a combination of the two, to clearly separate the component noise such as the aft fan and the jet components from the total. If this is feasible, the shielding characteristics of the noise components can then be studied, and the quantitative differences in the source ranking order and in the individual component characteristics between the demonstrator engine and the vision engine can be corrected by prediction tools.

To achieve this goal, the demonstrator engine needs to be characterized without the PAA installation effects that result from integration with the airframe. For this, the engine must first be tested in isolation on a static engine test stand with an inflow control device. This ground test, with the test conditions and environment controlled for best data quality, excludes the installation effects and flight effects associated with a flight test, and hence, can greatly facilitate the decomposition of component noise and source mechanisms. The decomposition process will rely on a combination of advanced measurements such as microphone phased arrays and analytical/prediction methods. The difference between the isolated and the flight test can then be used to quantify the PAA effects, as long as proper corrections are made to account for the flight effects on engine noise. Ideally, these flight effects could be dealt with by flight tests with conventional designs with the same engines mounted under the wing, but this extra step will have to depend on the availability of such an existing aircraft.

Given that it has been shown that the PAA effects are the single largest differentiating factor in advanced aircraft that are able to reach the NASA Mid Term and Far Term noise goals, measuring the PAA effects with the best available UHBP engine represents a unique opportunity to advance low noise aircraft maturation.

B. Noise Reduction Technologies

A second opportunity is to demonstrate noise reduction technologies that have been studied and shown to be important contributors to vision vehicles being able to achieve the NASA ARMD Mid Term noise reduction and even the Far Term noise reduction goal [3, 5, 6, and 18].

From the range of noise reduction technologies in the NASA portfolio, three are selected for this case study. These three technologies represent the concepts that have the most potential to reduce key noise sources on the airframe and could be applied to many of the candidate vision vehicles. In this case study, they are applied to the MFN airframe of the full fidelity vision vehicle and to the realistically scaled MFN airframes from Section V.B.

The pod gear is an approach to reducing main landing gear noise that is enabled by the unconventional airframes that generate the most favorable PAA effects; that is, the over-the-wing engine installation that is the single largest noise reduction approach. This also enables the pod gear to be applied to reduce the main gear noise. The pod gear has been described in Ref. 6 and applied to the HWB Far Term technology roadmap study [5] and to the MFN Far Term technology roadmap [18].

The Krueger flap was the leading edge device for all thirteen vehicles in the ERA Mid Term technology portfolio [3, 11] in order to enable the fuel burn reduction from laminar flow wings. The Krueger flap noise represents a new challenge that can be a significant contributor not only on approach but also at lateral and flyover conditions, depending on aircraft type [3, 5]. Therefore, NASA has developed the concept of a dual use fairing for the Krueger flap [5, 18] that fills the cove, reducing the noise from that subcomponent, and also partially covers the brackets reducing the noise from this other important subcomponent.
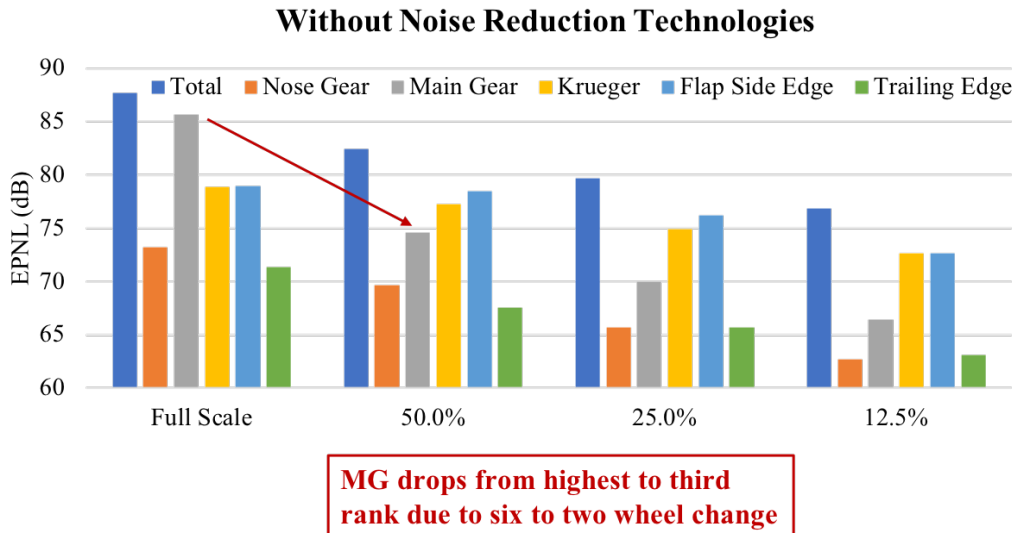
The most significant reduction of flap side edge noise has been considered to be a continuous mold line (CML) technology. Based on considerable experience, this concept was described in detail in Ref. 18 and applied to the MFN with a conservative implementation had a measured 6 dB peak noise reduction as compared to earlier, typically more aggressive, 10 dB peak noise reductions.

Fig. 20 quantifies the results for the airframes without noise reduction technologies applied. For the realistically scaled vehicles, the main gear is changed to a two wheel for 50% scale and below, and the leading and trailing edge devices have reduced complexity, as has been discussed previously. The total airframe noise is reduced, as expected, for the increasingly smaller scaled demonstrators. The change from six-wheel to two-wheel on the main gear creates a significant change in the ranking of the airframe sources. Main gear is the highest airframe source on the vision vehicle; however, on the 50% scaled vehicle, it is now the third in rank order of amplitude.
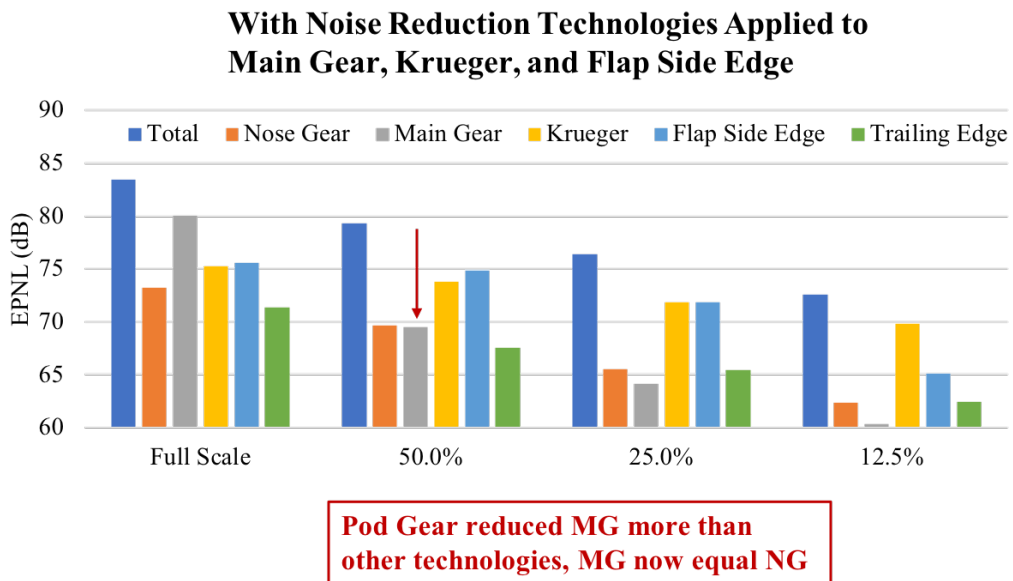
To successfully demonstrate in flight the noise reduction for a specific component, all the challenges listed previously still apply now with one important additional challenge; that is the phased array instrumentation must be

able to separate the components sufficiently (frequency range, polar angle range, and even, in some cases, azimuthal angle range) from other competing components, both with and without the noise reduction technology applied.

Fig. 21 shows the impact of applying all three technologies to the MFN airframes for all vehicles. In addition, the impact of each technology on the component is also evident. The pod gear is more effective at reducing main gear noise as compared to the dual use fairing on the Krueger flap or the CML on the flap side edge. This, together with the fact that the main gear was changed from a six wheel to a much quieter two-wheel main gear means that when the pod gear is applied the main gear is now more than 5 dB lower than both the Krueger and the flap side edge. The phased array must be capable of separating this very low main gear noise that is so low that it is even on the same order as the nose gear.

Without Noise Reduction Technologies

MG drops from highest to third rank due to six to two wheel change

Fig. 20 Predicted airframe noise components for the full scale MFN and the realistically scaled MFN airframes, approach condition.

With Noise Reduction Technologies Applied to Main Gear, Krueger, and Flap Side Edge

Pod Gear reduced MG more than other technologies, MG now equal NG

Fig. 21 Predicted airframe noise components for the full scale MFN and the realistically scaled MFN airframes, approach condition. Pod Gear applied to the main gear, Dual Use Fairing applied to the Krueger flap, and the CML applied to the flap side edge.

C. Flight Acoustic Instrumentation Discussion

Acoustic instrumentation for X-plane flight research is likely to be comprised of two main components. The first component is a set of conventional standalone microphones commonly used for noise certifications. Certification standards require these microphones to be placed on 4 ft stands to capture the effects of ground reflection that a person would experience while standing or sitting. This specification is intended to more closely model human perception of aircraft noise. However, ground reflections create an interference pattern in measured spectral levels that is a function of aircraft position. For acoustic flight research, where the intent is to measure and understand the sources of sound, the human perception effects are undesirable because they mask the true signal from the aircraft and must be removed during post-processing. As some uncertainty is inherent in this post-process, standalone microphones are most likely to also be placed on the ground to eliminate this interference pattern. Although ground reflections are still present, the direct and reflected ray paths are nearly equal leading to a simple pressure-doubling that can be easily corrected.

Although corrections for ground-board microphones are significantly simpler than for pole-mounted microphones, the ground-board microphones have additional challenges. Acoustic waves impinging on a surface can be scattered if the geometric features of that surface are of a similar size as the acoustic wavelength. For the small irregular surfaces near a microphone (mounting hardware, edges, etc.), this commonly occurs at high frequencies, and these scattered waves can contaminate the measured data. Ground-board microphones come in several variations, all related to the orientation of the microphones with respect to the board. Microphones may either be flush-mounted, inverted, or placed on their sides. Flush-mounted microphones, where the face of the microphone is placed flush with the top surface of the board, are preferable because they limit the amount of scattering geometry near the sensor. If flush-mounted microphones cannot be used or are unavailable, the microphones are inverted or placed on their sides, but again, this results in additional scattering geometry, which contaminates high-frequency noise. For microphones and ground boards commonly used in flight testing, this scattering begins to contaminate the noise spectra above approximately 5 kHz, where the acoustic wavelength is approximately 7 cm. As this frequency is set by the measurement system, and not by any characteristics of the aircraft (noise source), smaller scaled demonstrators are more susceptible to noise contamination, as the frequency range to be measured is higher, as discussed in previous sections.

As mentioned at the start of this section, there are two main components to acoustic instrumentation. The second component to be discussed is the microphone phased array. Phased arrays have been used extensively both in wind tunnel tests and in flight tests. They take advantage of coherent acoustic waves transmitted to multiple microphones to spatially isolate individual noise sources and determine the relative strengths of those sources, even if the source levels are below background noise levels. This is a critical tool for acoustic flight research, as it is the only way to measure the levels of individual aircraft components from a flyover of a full aircraft. Using a phased array, the relative strengths of landing gear noise, flap side edge noise, and slat noise, for example, can all be quantified, which is essential for validation and improvement of the individual methods and noise prediction models used to estimate the noise of a full aircraft. Phased array design is a complex, multifaceted process, and a full discussion of all possible parameters, trade-offs, and design choices is beyond the scope of this paper. The discussion to follow is meant to give an overview of basic array properties that are relevant to the early planning phases of X-plane acoustic flight research, considering questions of aircraft scale, overall array size, etc.

The usefulness of a phased array depends on its ability to adequately separate and measure the strength of individual sources. Two key descriptors of array performance in this regard are resolution and dynamic range. Resolution describes the array's ability to determine source location and is defined as the spatial extent of the "main lobe" of a beamform map, or more specifically, the point at which the spatial filter imposed by the array processing algorithm reaches a level that is 3 dB down from its peak [19]. The width of the main lobe (or "beamwidth"), and therefore the array's ability to resolve individual sources, is a function of the array aperture (physical diameter of the array) and the frequency in question. As array aperture and frequency increase, the resolution of a given array improves, that is, the beamwidth becomes narrower.

Although resolution improves as frequency increases, two other factors come into play at higher frequencies. The first is dynamic range. As wavelength decreases, spatial aliasing causes spurious lobes (called "sidelobes") to appear in the beamform map. This is illustrated in Fig. 22. As frequency is increased, wavelength shortens, and spatial aliasing has more effect on the beamforming results. As a result, maximum sidelobe level rises relative to the main lobe level. If the maximum sidelobe is 10 dB below the main lobe, the array is said to have a dynamic range of 10 dB at that frequency. In this case, the array will not be able to reliably identify and measure sources that are 10 dB quieter than the loudest source at that frequency, since it is impossible to distinguish sidelobes from true sources. This is an important consideration when choosing an X-plane scale, as changes in source ranking may make certain sources impossible to measure. For example, with a dynamic range of 10 dB, it can be seen from Fig.

21 that the true noise levels of the pod gear would be impossible to measure on a 25% scale demonstrator, as the level would be about 10 dB below that of the flap side edge.

a) f_0
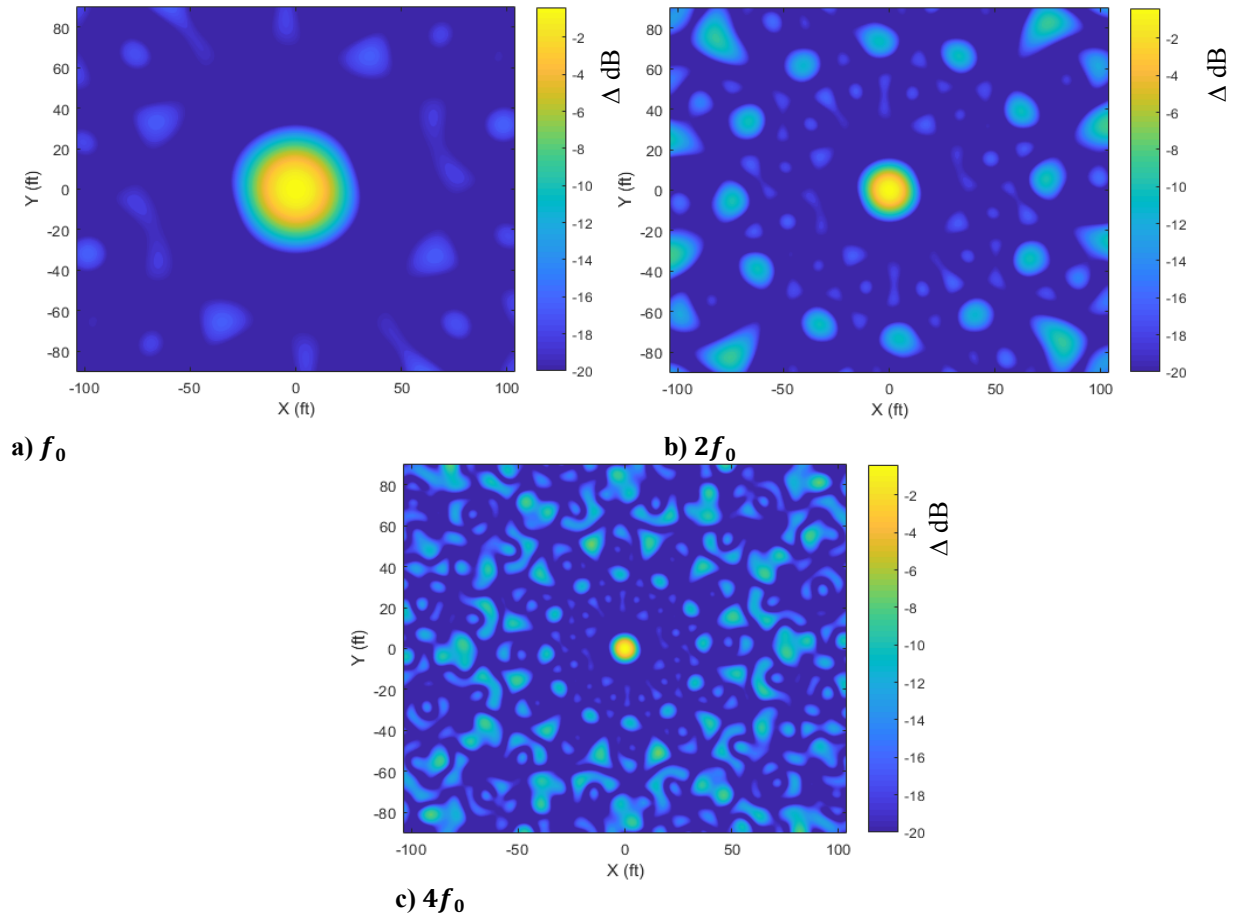
b) $2f_0$

c) $4f_0$

Fig. 22 Sample beamform maps of an ideal monopole source at a frequency of a) f_0, b) $2f_0$, and c) $4f_0$ showing the increasing presence of sidelobes at higher frequencies.

The other, more important factor to consider at higher frequencies is decorrelation of measured noise signals. At higher frequencies, as wavelength decreases, small variations in the propagation distances of acoustic waves as they travel between the source and the microphones break down the coherence of the signals between microphones. These variations may be caused by scattering from atmospheric turbulence or turbulent wakes shed from aircraft components. The effect of these variations is most easily seen in the time domain, but the result is equivalent in the frequency domain. Figure 23 illustrates the effect of a 3.4-cm (1.34 in) variation between the expected and acuatl propagation distances on the results of delay-and-sum beamforming. As seen in the figure, the 1-kHz result is not significantly affected by the change in propagation distance because the change is much smaller than the acoustic wavelength. However, the 5-kHz signal is completely nullified by the variation in propagation distance, which is one half-wavelength at this frequency. In an actual flight test, these variations in propagation distance would be randomly distributed both in time and among all microphones in the array, hence leading to an overall decorrelation of signal over the full array. Scattering from local geometry near the individual microphones, as discussed above in relation to standalone microphones, also contributes to decorrelation.
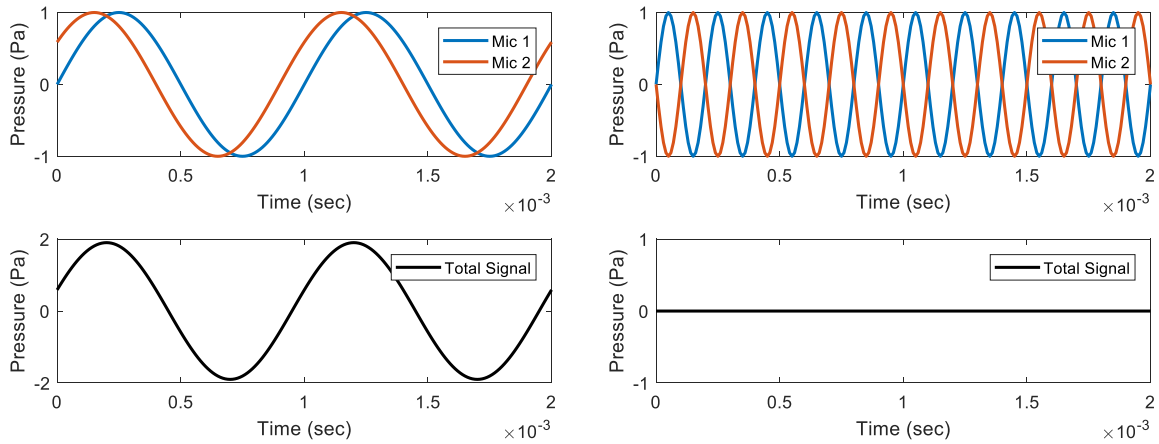
a) 1kHz   **b) 5 kHz**

Fig. 23 Illustrations of the effect of a 3.4-cm (1.34 in) variation in propagation distance on the results of delay-and-sum beamforming for a) 1 kHz and b) 5 kHz frequencies. The signal to Mic 1 follows the expected ray path, but the signal to Mic 2 follows a longer ray path than expected.

In wind tunnel testing, where the array is placed very close to the noise source, variations in total propagation distance are small, such that decorrelation only occurs at very high frequencies. However, in flyover-type measurements, where the minimum propagation distance is about 400 ft, these variations can grow and influence measurements at lower frequencies. Fig. 24 shows sample integrated spectra from flyover measurements along with the predicted noise spectra. Measurements largely agree with the predicted spectra at low frequencies, but decorrelation increases with frequency, eventually reaching a peak around 1 kHz for this case. Here, there is large uncertainty in the measurements, and levels are 5-10 dB below the expected value. At frequencies above 1 kHz, the spectra are dominated by semicoherent scattering effects from the microphone installation, leading to high spectral uncertainty.
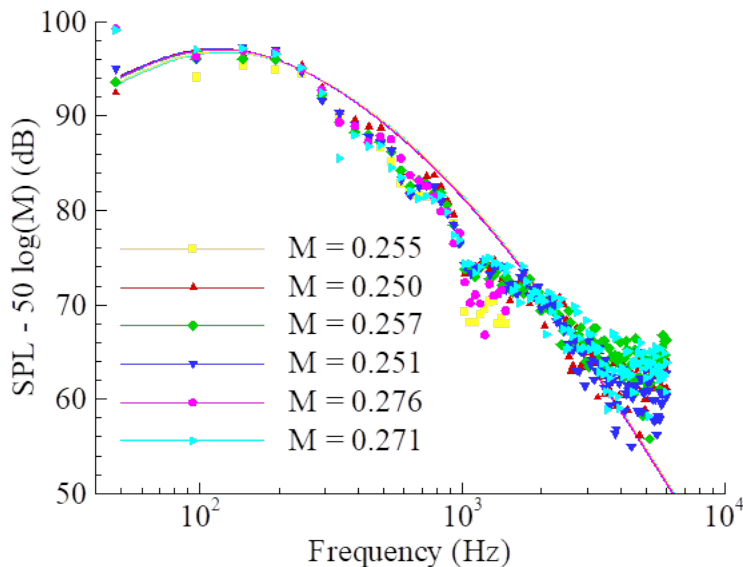
Fig. 24 Sample spectra calculated from integration of beamform maps obtained from flyover testing. The solid lines represent the ideal noise source spectra, while symbols indicate measured values. Reproduced from [20] with permission.

For X-plane demonstrator flight research, the array design will depend on the chosen scale of the X-plane. For this discussion, the full-scale array is assumed to have a similar design to that of Humphreys et al. [21], which

represents NASA's primary capability at the time of writing. It is possible to compare the performance of this array for various scaled MFN demonstrators. As the demonstrator is scaled down, the array is likewise scaled down by the same amount, i.e., for a half-scale demonstrator, the array aperture is half that of the full-scale array. This is done to mitigate problems associated with decorrelation as described above. The number of microphones is held constant. If the flyover distance is held constant at 400 ft for safety reasons, the beamwidth grows relative to the aircraft as scale decreases as seen in Fig. 25, which shows the ideal point spread function for a source near the main gear location. For the 100% and 50% demonstrators, the beamwidth at this frequency is sufficiently small such that source separation is possible for most locations on the aircraft. However, by 25%, the beamwidth is large, and it is expected that separation of flap and slat noise, for example, would be difficult.

a) 100%

b) 50%

c) 25%
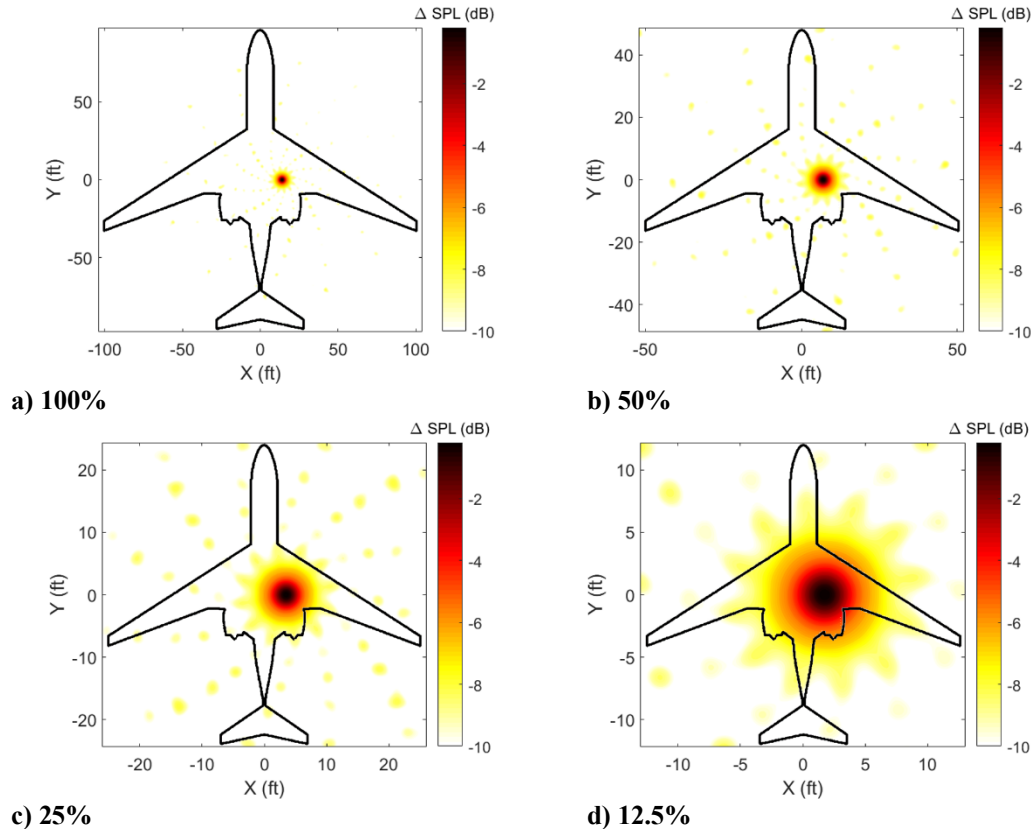
d) 12.5%

Fig. 25 Array point spread function for 1 kHz (full scale) overlaid on MFN outline for a) 100%, b) 50%, c) 25%, and d) 12.5% scale demonstrators.

It is important to note here that the plots in Fig. 25 do not include the effects of signal decorrelation, which is likely to degrade the signals at higher frequencies even if the overall array aperture is decreased. This is especially true if, again, the flyover distance is maintained at 400 ft for the reasons discussed above. The plots also do not consider the individual microphone characteristics. The array of Humphreys et al. [21] uses hardened, weather-proof microphones with a flat frequency response up to approximately 8 kHz. Above this frequency, resonance within the microphone causes wide variations in amplitude and phase response between microphones, making beamforming unreliable above this frequency without extensive calibration procedures. Fig. 25c (25% scale) represents a beamform image at 4 kHz, corresponding to 1 kHz full scale. To capture the full scale range of frequencies that have the most influence on PNLT and EPNL, the array would need to reliably beamform up to 4 kHz full scale, or 16 kHz for a 25% scale demonstrator. This is impossible for the present array, and would still be extremely difficult even with significant upgrades to the microphones due to the unavoidable presence of sidelobes and decorrelation effects. Even so, as discussed in previous sections, an ideal measurement system would be able to measure over the full range of frequencies (up to 10 kHz full scale) that contribute to PNLT and EPNL.

Some of the issues described above could be mitigated, but not eliminated, through the use of deconvolution methods for array processing, which can increase the resolution of array measurements. However, deconvolution is not a fix for poor experiment design, and the success or failure of deconvolution is entirely dependent on the quality of the collected data. The discussions here are meant to serve as a guide to issues that would impact the usefulness

of measured data for an X-plane demonstrator. In summary, a phased array for a flyover measurement performs best at low- to mid-frequencies, below approximately 4 kHz, due to the unavoidable effect of signal decorrelation due to acoustic scattering by atmospheric turbulence and microphone installation. X-plane scale determines the quality of acoustic data because beamwidth grows relative to the aircraft as scale is decreased, and because changes in relative source levels may make quieter sources indistinguishable from sidelobes of louder sources. Significant upgrades to the array of Humphreys et al. [21] would be necessary to obtain data up to 10 kHz full scale, including higher-quality microphones that can reliably measure up to 10 kHz in their passband, as well as a higher channel count.

D. Significant Additional Opportunities

There are significant additional opportunities for X-plane acoustic flight research. These will be mentioned briefly here but not thoroughly developed.

The most obvious opportunity created by an X-plane is to flight test technologies in addition to those initially considered in scope of an X-plane. The X-plane could be used as a testbed for these technologies, the results of which could be factored into predictions of vision vehicles of different technology levels. The pod gear, the Krueger dual use fairing, and the CML flap are three airframe noise reduction technologies listed in this paper that are examples of technologies that could be designed into an X-plane for the initial flight campaign or that could be added on subsequent flight campaigns.

Even with an X-plane using an off-the-shelf engine, there are now engines on the market that are ultra high bypass ratio, ~12, and that are also geared fans. These engines are more representative of future engines of even higher bypass ratio, ~15 to ~20, as compared to many of the other available older generation commercial-off-the-shelf engines. The acquisition of high quality acoustic data from a static engine test would improve prediction methods for total engine levels, directivity, and engine source ranking. Having isolated static engine data together with flight data of the vehicle with the same engine would then improve the prediction of the PAA effects and flight effects for the engine sources.

Cumulative EPNL below the regulatory limit is the metric that NASA uses for the aircraft system level measure. Ultimately, the broader goal is for reduced population exposed to objectionable noise levels. Thus, in addition to predicting the cumulative noise metric, predicting the ground noise contour of noise for an aircraft at landing and takeoff is also a key capability. These Mid Term and Far Term aircraft concept configurations introduce significant azimuthal directivity from PAA effects and even from the installation effects of the airframe sources, and have much lower noise levels than current aircraft. Ground contours also involve propagation over longer distances, a problem that has already been mentioned. Acoustic flight research that includes accurate azimuthal directivity measurements and longer range measurements represents a unique opportunity to improve the prediction of ground contours with a direct impact on the ability to more accurately quantify the noise reduction impact on the community.

VII.   Possible Alternative Approaches

This paper has outlined many of the relevant challenges and opportunities to reach the goal of successful acoustic flight research of advanced aircraft configurations and technologies. Improved instrumentation capabilities and innovative flight test procedures are some approaches that have been mentioned as necessary. It is also important to mention that there are alternative approaches that are conceivable that may be able to overcome some of the significant challenges and add value to the research. Some ideas include:

- Chase airplanes carrying instrumentation,
- Goal post towers to hold arrays of microphones and,
- A static airplane acoustic test (with ICDs on the engine intakes), analogous to a static engine test.

Each idea would require extensive investigation and design and at the conclusion of that investigation may not, in fact, prove out to be a valuable alternative.

Another alternative is to use existing aircraft as experimental flight test beds. This approach has been used successfully many times. The Boeing led Quiet Technology Demonstrator 2 [22] and the more recent Boeing EcoDemonstrator projects have been very productive flight test demonstrations of a variety of noise reduction technologies [22] including PAA technology [23]. The advantages of this approach certainly include the ability to test technology at full scale, high geometric fidelity, and with flight effects. Obviously, it can become more challenging to use an existing aircraft to test technologies that rely on a different configuration, the pod gear for example. In addition, testing the configuration PAA effects of an advanced configuration concept such as the MFN on an existing aircraft test bed such as a B777 would also be challenging, at the least.

VIII.   Conclusions and Recommendations

Due to the many interrelated elements, the design of an X-plane demonstrator, selected technologies, and the acoustic flight research must be carefully analyzed and designed in order to create a sound plan to accomplish the overall acoustic objectives related to the noise goal. A process has been developed and demonstrated in this paper for the formulation of the acoustic research of an X-plane. The many interrelated elements are identified that influence the acoustics of the X-plane.

In general, acoustic flight research with an X-plane demonstrator is seen as most directly valuable if the scale factor can be kept above 75% where it is likely that the many interrelated elements can be addressed successfully. A demonstrator of 50% scale of the vision aircraft is the lowest scale factor advisable. As the scale factor approaches 50%, technical limitations become more severe and must be more carefully considered from the beginning of the design of the X-plane, technologies, flight research objectives and, certainly in the data analysis.

Using the formulation process developed in this research, additional analysis cycles can produce more specific recommendations of acoustic objectives, scale factor, technologies, and flight research plans.

As the size of the vision vehicle increases, clearly a large scale factor is likely to become more costly. For the scenario that the vision vehicle is a single aisle replacement, 160-230 passenger range, then a scale factor above 75% should be more cost effective to achieve. This will mitigate the issues around frequency scaling; however, geometric fidelity, for example, are among factors that still must be carefully considered.

The issues of the geometric fidelity of the demonstrator's components as they relate to the complexity of the vision vehicle must be carefully understood and accounted for in the use of the data to support the predictions for the vision vehicle. Efforts should be made to increase the geometric fidelity on the scale demonstrator for those selected technologies and components that are central to the acoustic flight research. This is especially true for key noise reduction technologies, designs, or features.

Scale factors below 50% are not completely eliminated. It is conceivable that with innovative approaches there may be some very specific and limited information obtained that may support, albeit more indirectly, the overall objectives. This should be considered only if no higher value alternatives are possible.

Quantification and measurement of the PAA effects over the range of important polar and azimuthal angles is essential in order to determine this most important acoustic impact of an advanced unconventional aircraft configuration. The value is greatest with the selection of a demonstrator engine that is representative of future, UHBP engines in terms of source ranking and directivity characteristics.

Isolated engine measurement as part of an X-plane acoustics campaign would be very valuable to the overall objectives. Source separated isolated engine data can be very useful for improving the engine noise prediction, as well as for the purpose of quantifying the PAA effects.

It is likely that NASA's instrumentation capabilities will need to be significantly increased due to the requirements for scaled vehicle flight research. The demonstration of individual noise reduction technologies will depend on the phased microphone array's ability to identify and quantify the source. This ability degrades at high frequencies due to the governing physics of array processing, which would have more impact on small scale demonstrators. The microphone count of the array in addition to the frequency range of the individual microphones will be particularly important.

Site selection should include documentation of ambient wind, temperature, humidity, background noise, and the operational environment, all of which can significantly impact or limit the flight acoustic research.

Overall, the acoustic flight research of an X-plane represents a great opportunity to investigate the transformative impact of aircraft configuration change, innovative noise reduction technologies, and flight test methods and instrumentation.

Acknowledgments

References

1. Thomas, R.H., Burley, C.L., and Olson, E.D., "Hybrid Wing Body Aircraft System Noise Assessment with Propulsion Airframe Aeroacoustic Experiments," *International Journal of Aeroacoustics*, Vol. 11 (3+4), pp. 369-410, 2012.
2. Czech, M.J., Thomas, R.H., and Elkoby, R., "Propulsion Airframe Aeroacoustic Integration Effects of a Hybrid Wing Body Aircraft Configuration," *International Journal of Aeroacoustics*, Vol. 11 (3+4), pp. 335-368, 2012.
3. Thomas, R.H., Burley, C.L., and Nickol, C.L., "Assessment of the Noise Reduction Potential of Advanced Subsonic Transport Concepts for NASA's Environmentally Responsible Aviation Project," AIAA Paper 2016-0863.
4. Thomas, R.H., Burley, C.L., and Guo, Y., "Progress of Aircraft System Noise Assessment with Uncertainty Quantification for the Environmentally Responsible Aviation Project," AIAA Paper No. 2016-3040.
5. Thomas, R.H., Guo, Y., Berton, J.J., and Fernandez, H., "Aircraft Noise Reduction Technology Roadmap Toward Achieving the NASA 2035 Noise Goal," AIAA Paper No. 2017-3193.
6. Thomas, R.H., Nickol, C.L., Burley, C.L., and Guo, Y., "Potential for Landing Gear Noise Reduction on Advanced Aircraft Configurations," AIAA Paper 2016-3039.
7. Collier, F.S. and Wahls, R.A., "NASA Aeronautics Strategic Implementation, Strategic Thrust 3A Roadmap Overview, Ultra-Efficient Commercial Vehicles – Subsonic Transports," NASA Aeronautics Research Mission Directorate presentation, June 1, 2016, www.nasa.gov, accessed June 16, 2016.
8. Thomas, R.H. and Guo, Y., "Ground Noise Contour Prediction for a NASA Hybrid Wing Body Subsonic Transport Aircraft," AIAA 2017-3194.
9. Bonet, J.T., Schellenger, H.G., Rawdon, B.K., Elmer, K.R., Wakayama, S.R., Brown, D. and Guo, Y.P., "Environmentally Responsible Aviation (ERA) Project – N+2 Advanced Vehicle Concepts Study and Conceptual Design of Subscale Test Vehicle (STV)," NASA Contract Report 2013-216519, 2013.
10. Guo,Y.P., Nickol, C.L., and Thomas, R.H., "Noise and Fuel Burn Reduction Potential of an Innovative Subsonic Transport Configuration," AIAA Paper 2014-257.
11. Nickol, C.L. and Haller, W.J., "Assessment of the Fuel Burn Reduction Potential of Advanced Subsonic Transport Concepts for NASA's Environmentally Responsible Aviation Project," AIAA Paper 2016-1030.
12. Guo, Y., Burley, C.L., and Thomas, R.H., "Landing Gear Noise Prediction and Analysis for Tube-and-Wing and Hybrid Wing Body Aircraft," AIAA Paper 2016-1273.
13. Guo, Y., Burley, C.L., and Thomas, R.H., "Modeling and Prediction of Krueger Device Noise," AIAA Paper 2016-2957.
14. Bass, H. E., Sutherland, L.C., Piercy, J., and Evans, L. *Absorption of sound by the atmosphere*. Physical Acoustics: Principles and methods*, pp. 145-232,. Vol. 17. 1984.
15. Society of Automotive Engineers. *Standard Values of Atmospheric Absorption as a Function of Temperature and Humidity*. Aerospace Recommended Practice 866A, March 1975.
16. American National Standards Institute. *Method for Calculation of the Absorption of Sound by the Atmosphere*. ANSI S1.26-2014, August 2014.
17. Montegani, Francis J. *Computation of Atmospheric Attenuation of Sound for Fractional-Octave Bands*. NASA TP-1412, February 1979.
18. Guo, Y., Thomas, R.H., Clark, I.A. and June, J.C., "Far Term Noise Reduction Roadmap for the Mid-Fuselage Subsonic Transport," AIAA paper to appear, AIAA/CEAS Aeroacoustics Conference, June 2018.
19. Mueller, T. J., *Aeroacoustic Measurements*, Springer, Berlin, 2002.
20. Guo Y. P. "Airframe Noise Prediction by Acoustic Analogy" *Von Karman Institute Lecture Series*, March 2009.
21. Humphreys, W. M., Lockard, D. P., Khorrami, M. R., Culliton, W., & McSwain, R., "Evaluation of Methods for In-Situ Calibration of Field-Deployable Microphone Phased Arrays", *23rd AIAA/CEAS Aeroacoustics Conference,* Denver, Colorado, AIAA Paper 2017-4176.
22. Herkes, W.H., Olsen, R.F., and Uellenberg, S., "The Quiet Technology Demonstrator Program: Flight Validation of Airplane Noise-Reduction Concepts," AIAA-2006-2720.
23. Nesbitt, E., Mengle, V., Czech, M., Callender, B., and Thomas, R., "Flight Test Results for Uniquely Tailored Propulsion Airframe Aeroacoustic Chevrons: Community Noise," AIAA-2006-2438.